Daytime climatology of ionospheric N_mF_2 and h_mF_2 from COSMIC data

A. G. Burns,[1] S. C. Solomon,[1] W. Wang,[1] L. Qian,[1] Y. Zhang,[2] and L. J. Paxton[2]

Received 17 January 2012; revised 13 July 2012; accepted 20 July 2012; published 22 September 2012.

[1] Constellation Observing System for Meteorology, Ionosphere and Climate (COSMIC) data were analyzed to study the climatological variations of the F_2 region ionosphere. A 30 day running median was applied to the daily medians of each geomagnetic latitude bin (10^0) to remove the short-term variability of the data. This permitted a better description of the long-term daytime climatology across the most recent solar minimum to be obtained. Several significant features appeared in this climatology: 1) low-latitude N_mF_2 was dominated by the semi-annual anomaly, the equatorial anomaly and the annual asymmetry (anomaly); 2) Semi-annual and annual anomalies extended into the middle latitudes; 3) this extension into the middle latitudes appears to be dependent on variations of solar radiation over the solar cycle, as the variations did not reach as far poleward in 2008 as they did in 2010; 4) The second equinoctial maximum is not centered on the September equinox, but occurred in October; 5) there is an annual variation at high latitudes in which maximum values of N_mF_2 occur in summer – there is no indication of a winter anomaly and, in fact, when hemispheres are compared, maximum N_mF_2 at middle latitudes always occurs in the summer hemisphere rather than the winter one; 6) the highest values of h_mF_2 at low latitudes occur on the summer side of the magnetic equator throughout the four year period, probably resulting from winds blowing from the summer to the winter; 7) minimum values of h_mF_2 at middle latitudes occur in winter, when h_mF_2 is typically 30 to 50 km lower than it is in summer; 8) elevated h_mF_2 also occurs in summer at high latitudes, with a distinct seasonal and hemispheric asymmetry.

Citation: Burns, A. G., S. C. Solomon, W. Wang, L. Qian, Y. Zhang, and L. J. Paxton (2012), Daytime climatology of ionospheric N_mF_2 and h_mF_2 from COSMIC data, *J. Geophys. Res.*, *117*, A09315, doi:10.1029/2012JA017529.

1. Introduction

[2] Our understanding of F_2 region climatology has been built up by numerous experiments that have been described in the literature over the past 70 or 80 years and is probably best expressed in the IRI model [*Bilitza and Reinisch*, 2008]. Several salient features of the ionosphere diverge considerably from a simple solar-zenith-angle-controlled F_2-region ionosphere. These features include: the equatorial anomalies, which are two bands of increased electron density 15 to 20 degrees on either side of the geomagnetic equator [e.g., *Appleton*, 1946] (for modern references see *Ram et al.* [2009]); the winter anomaly in which electron densities are greater at middle latitudes in winter than in summer [*Berkner et al.*, 1936] (see *Rishbeth* [1998] for modern references); the annual asymmetry or anomaly [*Berkner et al.*, 1936] (see *Rishbeth* [1998] for modern references) in which electron densities are greater in the December solstice than they are in the June solstice; and the equinoctial maxima of N_mF_2 where electron densities are greater in the equinoxes than they are in summer and winter [*Berkner et al.*, 1936] (see *Rishbeth* [1998] for modern references). There is a further anomaly, the Weddell Sea anomaly [*Bellchambers and Piggott*, 1958], or as we call it the Summer Evening Anomaly [e.g., *Burns et al.*, 2008, 2011] in which electron densities are greater at night than during the day at certain locations, but this does not appear in the global averages described here, so we will not discuss it further.

[3] Much of the work that has gone on in understanding the thermosphere and ionosphere in the intervening 70 years has involved developing explanations for these phenomena and extending it to other, usually shorter-term, variations of the thermosphere and ionosphere, like geomagnetic storms. One example of the development of ways to explain these phenomena involves the winter or seasonal anomaly. *Rishbeth and Setty* [1961] suggested that the winter or seasonal

[1]High Altitude Observatory, National Center for Atmospheric Research, Boulder, Colorado, USA.
[2]Applied Physics Laboratory, Johns Hopkins University, Laurel, Maryland, USA.

Corresponding author: A. G. Burns, High Altitude Observatory, National Center for Atmospheric Research, Boulder, CO 80307–3000, USA. (aburns@ucar.edu)

0148-0227/12/2012JA017529

anomaly was caused by changes in neutral composition, although the nature of the morphology of thermospheric composition was not well known at the time. The seasonal distribution of neutral composition was only firmly established in the 1970s [e.g., *Prölss and von Zahn*, 1974], but it was found to be in general agreement with the composition structure postulated by *Rishbeth and Setty* [1961].

[4] The explanations for this and all the other anomalies, apart from the equatorial anomalies, were summarized by *Rishbeth* [1998]. *Rishbeth* [1998]'s discussion of the equinoctial anomalies is summarized in the discussion section as it pertains to the observations that are presented here. Recent work [*Zeng et al.*, 2008] has indicated that the annual asymmetry or anomaly is a geometric result of the displacement of the geomagnetic poles relative to the geographic ones and the consequent location of the geomagnetic equator, so that the summer ionosphere sees more illumination in the December solstice than in the June one. Current thinking on the equatorial anomalies is that they are caused by the equatorial fountain [*Schunk and Nagy*, 2000]. Our understanding of these anomalies is based on data that have been collected over the last 70 years. It is worthwhile describing these data here and investigating how the data set used in this paper differs from these previous data sets.

[5] The first data used to investigate the ionosphere came from ground based radars [e.g., *Appleton and Barnett*, 1925] and particularly from what are now called ionosondes. Initially there were very few of these, a fairly large number were installed in the 1950s and 1960s and then the numbers decreased again in the following decades as other experiments gained popularity. They had the great advantage of being relatively cheap and thus relatively widespread, but they had the disadvantage that they could only be installed on land and were found in the relatively few countries that supported ionospheric research. Thus, their distribution has always been somewhat limited. Another form of ground based radar is the Incoherent Scatter Radar [e.g., *Evans*, 1965]. These are expensive and therefore rare. While they give a great deal of information about the local ionosphere, their ability to provide a global morphology is limited by the small number of stations. A third ground-based radio technique that has developed in recent years is the use of dual frequency GPS (Global Positioning System) observations [e.g., *Coster et al.*, 2003] from the ground. These provide total electron content (TEC) measurements over much of the Earth's land surface, but the effects of changes in the top side scale height cannot be separated from those in N_mF_2. This inability to separate the two parameters is important because they have different responses to forcing as the topside scale height should be primarily temperature dependent, whereas the N_mF_2 changes are primarily affected by composition, winds and electric fields.

[6] A large number of space based measurements of electron density have also been made. Topside sounders like ISIS and Alouette [*Chapman*, 1964] made many measurements of the topside ionosphere from the 1960s to the 1980s, but most of the profiles from these missions had not been analyzed to provide electron densities [*Huang et al.*, 2002] until recently and thus they have not been fully used to develop climatologies. Their duty cycles were also limited. Langmuir probes [e.g., *Brace*, 1998] were also flown from the 1960s onward. These have provided in situ measurements of electron density, but have not readily provided information about the height of the F_2 peak or the electron densities there, as in situ measurements can give little information about where the F_2 peak is relative to the height of the satellite. These measurements are also along the satellite track only, so climatological studies can also suffer through the inability to uniquely separate local time and longitude effects and from satellite precession. In the last two decades, space based GPS observations have been made to improve meteorology, ocean sounding and ionospheric physics [e.g., *Yunck et al.*, 2000]. They too are restricted to the satellite track, so globally averaged climatologies cannot be obtained on time scales of days and weeks from a single satellite, and thus climatologies are difficult to construct using these data.

[7] In this paper, we use a new global ionospheric data set from COSMIC satellite radio occultation observations. COSMIC data [*Lei et al.*, 2007] come from measurements of GPS signals made from 6 Low Earth Orbiting (LEO) satellites across the Earth's limb. Two to three thousand measurements are made per day, which is sufficient to provide globally averaged N_mF_2 and h_mF_2 measurements for specific latitude and local time bins. The ambiguity between local time, universal time and longitude is thus significantly reduced, so improved climatology maps can be made. Results from this climatology are presented for daytime observations in this paper. The nighttime observations are sufficiently different that they will be reported in a later paper.

[8] The paper is organized in the following way. Section 2 gives a more detailed description of the COSMIC mission. Results are described in Section 3. These results are discussed in Section 4 and conclusions are drawn in the last Section.

2. The Data

[9] Six satellites, which are together called COSMIC, were launched on April 15, 2006 [*Kumar*, 2006]. Three different instruments make up their science payload. The instrument that interests us here is the advanced GPS receiver. It is used to make the atmosphere and ionosphere measurements through phase and Doppler shifts of radio signals. The phase advance is used to compute the amount of signal bending that occurs as the impact parameter varies [*Rocken et al.*, 2000]. This bending is then used to compute vertical profiles of refractivity. The refractivity is directly proportional to ionospheric electron densities when impact parameters are above 80 km [*Lei et al.*, 2007]. The Abel inversion technique is then applied to retrieve electron density profiles from the total electron content along these raypaths [*Hajj and Romans*, 1998; *Schreiner et al.*, 1999].

[10] The satellites were launched from the same rocket and initially followed the same orbit track at 512 km. The satellites were then sequentially raised to orbits at 800 km. The time delay for this increase in elevation was designed to spread the orbital planes, so the individual satellites are now 60 degrees apart. The COSMIC satellites continue to provide approximately 24 h of local time coverage globally and provided about 2000–2500 vertical electron density profiles per day during the period covered here.

[11] The data used in this study were retrieved from the COSMIC (http://www.cosmic.ucar.edu) observations from the beginning of 2007 until the end of 2010. Abel inverted

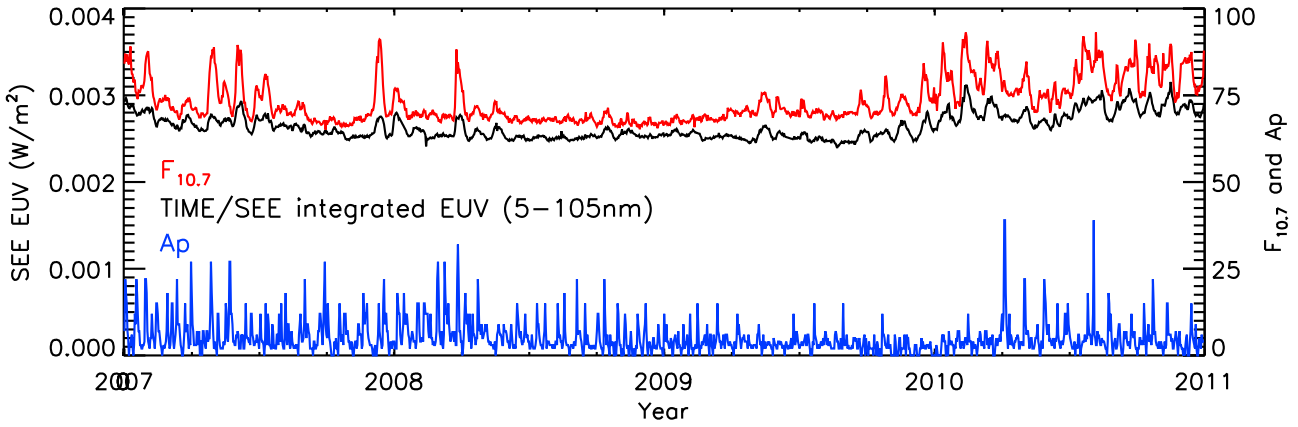

Figure 1. Variations in F10.7, solar EUV flux and kp during the period 2007–2010.

data [*Lei et al.*, 2007] were used in this study to obtain values for NmF_2 and hmF_2. The median of these N_mF_2 values was calculated for all local solar times between 0900 and 1500 for all longitudes and 10 degree bins in geomagnetic latitude, calculated using APEX coordinates [*Richmond*, 1995]. A 30-day running median was then applied to each magnetic latitude bin over the 4 years of the study to remove the day-to-day variability. Local times were selected to ensure that the ionosphere was mostly illuminated in both summer and winter. Other local time bins were tested including 1000–1400 and 0600–1800 and the results were qualitatively the same. Typically over 50 points occurred in low latitude bins for each day, so the 30 day running median meant that of the order of 1500 points occurred in each bin at low latitudes and about 750 points near 60 degrees. Longer bins were not used in case the results were affected by nighttime data.

[12] The variability of the NmF_2 and hmF_2 data for each bin have been calculated using the median absolute deviation (MAD) [*Hoaglin et al.*, 1983] for the COSMIC NmF_2 and hmF_2 for each bin on each day. This quantity is expressed as MAD = median(abs((value) - median(value))). This is a more robust measure of variability than standard deviations as outlying points do not have a disproportionate influence on the results. It gives the variability at periods of less than a day. A 30 day moving median has been applied to the results to smooth out short-term variations. These uncertainties are plotted only every 3 months on Figures 4 and 5, to keep the figures readable. The repeatability of the uncertainties in each season from year to year suggests an underlying geophysical cause of much of the uncertainty, perhaps because of changes in NmF_2 and hmF_2 over the 6 h from 0900 LT to 1500 LT.

[13] Strong horizontal gradients can cause the inversion to break down. So, for example, they would be expected to break down equatorward of the equatorial anomalies [*Yue et al.*, 2010] and effectively smear out the densities between the anomalies and the magnetic equator. The authors of this paper were surprised when this did not happen with these results, but no discussion of the behavior at low magnetic latitudes is included in this paper for this reason. There are also problems trying to apply Abel inversions below the F_2 peak (or in more general terms, to produce profiles below the brightest emission region when the inversion is applied from above). For this reason this study has concentrated data in regions where Abel inversions produce accurate results.

3. Results

[14] Figure 1 shows the variations in F10.7, solar EUV flux and kp during the period 2007–2010. There is no indication of regular forcing that might explain the semiannual and annual structures seen in the next two figures in this plot. The scale chosen for F10.7 and EUV radiation hides the continuing decrease of EUV radiation, but not F10.7, into 2008 that was discussed by *Solomon et al.* [2012].

[15] Figure 2 shows the median values on N_mF_2 calculated for local times 0900–1500. Weakest low latitude electron densities occurred in the second half of 2008 and the first half of 2009, when EUV measurements also indicated that solar radiance was at its lowest for this solar cycle [*Solomon et al.*, 2010]. Electron densities in both the tropics and the middle latitudes indicated that there had been a gradual decline in N_mF_2 from the beginning of 2007 to this minimum and then a rapid increase in N_mF_2 through to the end of 2010.

[16] A number of other features appear in this plot. The equatorial anomalies clearly occur throughout the period of study. The separation between them is constant within the constraints of the 10 degree magnetic latitude bin, indicating that if there is any change in the globally averaged separation with season, year or solar cycle, it is smaller than 10 degrees. The equatorial anomalies are saturated in 2010 to permit comparisons with other years, but when this saturation is removed they again appear at the same magnetic latitudes.

[17] Equinoctial maxima at low latitudes are a strong feature of these plots. Every year N_mF_2 is greater near the equinoxes than it is in either of the solstices, both in the low and middle latitudes, although the latitudinal extent of these effects varies over the 4 year time span, reaching a greater latitudinal extent in those years when there was stronger EUV radiation (2007 and 2010). The peaks do not occur right at the equinoxes: the peaks occur in March and October. There are indications that there may also be an asymmetry between the equinoxes, with greater values occurring in the March equinox, but this finding is problematical as these effects are largely masked by EUV radiation variations. The duration of these peaks is uncertain

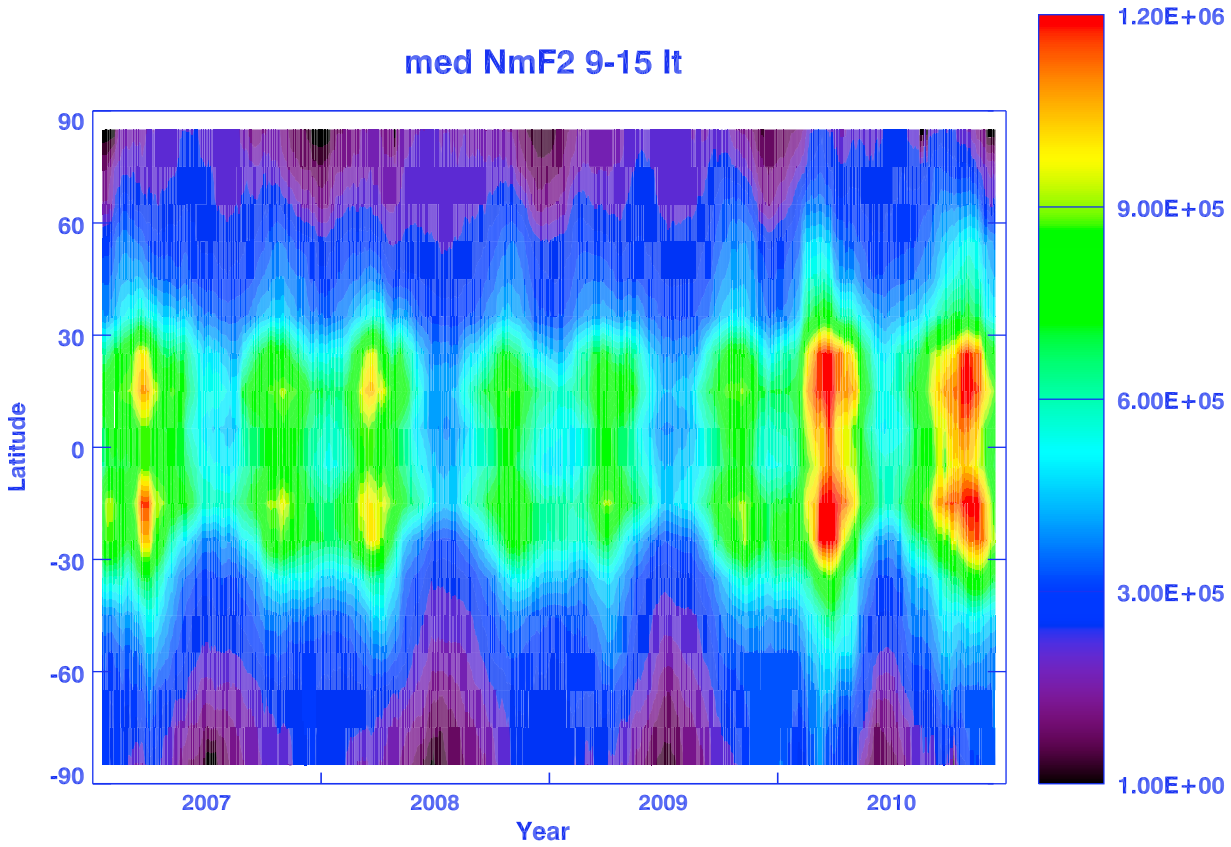

Figure 2. N_mF_2 climatology for 2007 to 2010 in magnetic latitude bins. Units are in per cubic centimeters. Each bin is calculated using the median of data from all longitudes for local times between 0900 and 1500 local solar time. The data were then further processed by taking a 30 day running median for each bin to remove short-term variability like geomagnetic activity and any possible short-term "breathing" modes of the atmosphere.

because the 30 day running median used and the smoothing done in contouring the results tends to smooth them out.

[18] The annual asymmetry or anomaly of N_mF_2 occurs at both low and middle latitudes, although again the latitudinal extent of this phenomenon varies over the four years of the study. December values of N_mF_2 are significantly greater than June values every year, typically being at least 20–40% greater.

[19] The high latitudes show a pattern that is expected if the controlling mechanism for N_mF_2 changes was the solar zenith angle. N_mF_2 is greatest in summer (June in the north and December in the south – the latter is represented by the dash that marks the boundary between years) and least in the winter, although there are shorter term variations as well (like the summer variations in the southern hemisphere).

[20] The variations of the annual asymmetries and the equinoctial maxima over the four year study period merit further description. The latitudinal extent of these variations is least in the minimum period from late in 2007 to the second half of 2009. Annual asymmetries and equinoctial maxima were seen at somewhat higher latitudes in early 2007 and much higher latitudes in late 2009 through 2010.

[21] A feature that is missing from this plot is the winter anomaly, using the definition that the winter anomaly is that condition in which N_mF_2 is greater in the winter hemisphere than in the summer hemisphere at a particular time in the middle latitudes. For all solstice days the summer N_mF_2 values are greater than the winter ones poleward of the equatorial anomalies for the same magnetic latitude bin. This will be considered further in the discussion section as the definition of the winter anomaly may cause some confusion.

[22] Figure 3 is the equivalent plot for h_mF_2. Note that the 30 day running median "smears out" the equinox transition, which is in reality much sharper than this and which will also be the subject of a subsequent paper. Several salient features appear in this plot. The most noticeable feature is the high values of h_mF_2 which occur near the magnetic equator. In this region the maximum values of h_mF_2 always occur on the summer side of the magnetic equator, producing a pronounced annual variation of h_mF_2. Equinoctial values of h_mF_2 are also lower than solstice values in this low latitude region.

[23] Annual variations of h_mF_2 are also dominant in the middle latitudes, with summer values typically being some 30 or 40 km higher than winter ones. There are also indications of an annual or hemispheric asymmetry at middle latitudes. Southern winter values of h_mF_2 are lower than those of the northern hemisphere in winter, but higher when summers are compared. Another way to state is that the annual variation in F_2 peak heights is much greater in the southern hemisphere than in the northern hemisphere.

[24] The situation at the very highest latitudes is more complicated and it may be contaminated by some of the

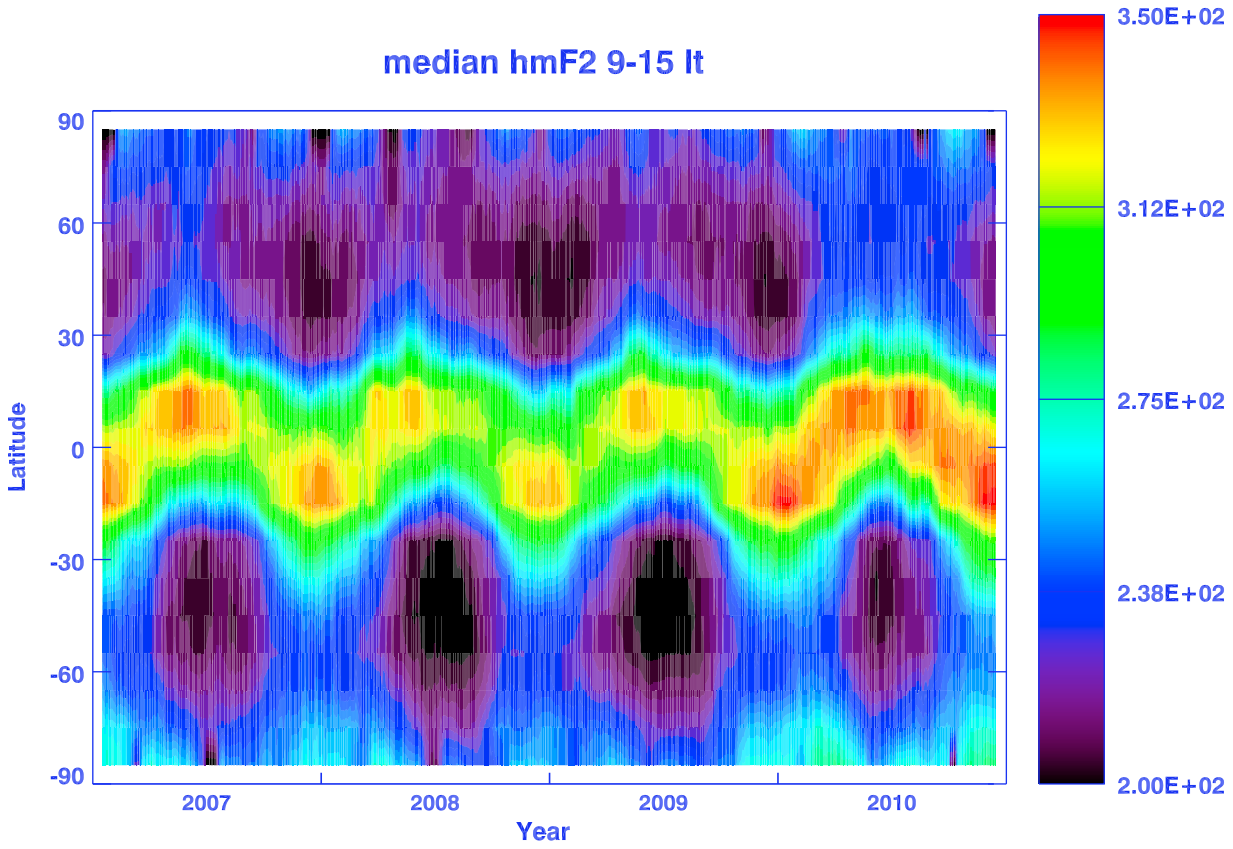

Figure 3. h_mF_2 climatology for 2007 to 2010 in magnetic latitude bins. Units are in kilometers. The data were processed in the same way that the N_mF_2 data were analyzed.

winter data being measured in places where the ionosphere is not illuminated and also lack of sufficient data coverage. There is a distinct annual effect in the southern high latitudes, with higher values of h_mF_2 occurring in the southern summer and lower values in winter. The changes in h_mF_2 in the northern high latitudes appear to be dominated by short-term variability. h_mF_2 is also higher in the southern high altitudes than it is in the northern high latitudes.

[25] There appear to be differences in the morphology of h_mF_2 going into 2010, but this may just reflect the generally greater heights of the F_2 layer as EUV radiance increases. However, it is interesting to note that these changes in morphology correspond to increases in the latitudinal extent of the annual asymmetry and the equinoctial maxima.

[26] Figure 4 gives line plots of N_mF_2 for 4 selected magnetic latitudes to illustrate the main features in Figure 2. At low latitudes (25 magnetic) the temporal changes are dominated by the semiannual variations, although there is also of a strong annual variation. The hemispheric difference associated with this annual variation is much stronger in December than in June and thus much greater in the south than in the north. At high latitudes (75 magnetic) the dominant feature is an annual variation, with a peak occurring in the summer in both hemisphere, although there is evidence of a small contribution from the semiannual oscillation (anomaly) in some years. Generally N_mF_2 is much smaller at high magnetic latitudes than low ones.

[27] Line plots for h_mF_2 are given in Figure 5. Three of the lines (25 degrees north and south and 75 degrees south magnetic) are dominated by an annual variation, with peaks occurring in midsummer when the Sun is at its highest point. Amplitudes of this variation are very similar at 25 north and 25 south, being of order of 80 to 90 km. The variation at 75 degrees south is smaller (around 40 km), but it is phase with the variation 25 degrees south. There is no clear pattern in the variation of hmF2 at 75 degrees north, but the variation is less than 20 km in total.

[28] Figures 6 and 7 show N_mF_2 in two different longitude sectors 90–180 and −180––90 respectively. Latitude bins have been extended to 15 degrees to accommodate the sparser data density. The two plots, as do the other two longitude sectors (not shown), preserve the features of the zonally averaged N_mF_2 plot (Figure 2) with minor changes that should be expected for two different longitude sectors. The most notable changes occur at high latitudes. There is a black band in the highest latitudes of the northern hemisphere in Figure 6. At these latitudes no geographic latitudes correspond to the magnetic latitudes, so no data are present in this longitude band. There is a similar band in the high southern latitudes in Figure 7 as there was no data available in the highest latitudes of the southern hemisphere at these longitudes. Equatorward of these high latitude features the annual structure that was discussed with respect to Figure 2 occur. In both cases the semiannual variation does not extend to such

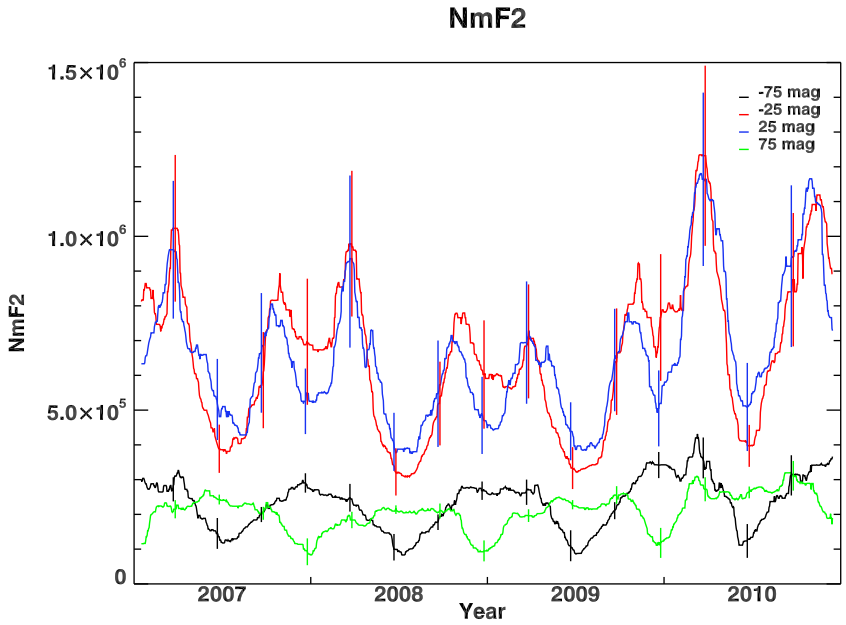

Figure 4. Line plots of N_mF_2 for four selected magnetic latitudes for the years 2007–2010. The vertical bars represent uncertainties calculated using MADs (see Section 2).

high latitudes in 2008 and 2009 as it does in 2010. The magnitude of the annual oscillation (anomaly) varies somewhat with longitude, although the change is not large. There is no evidence of a winter anomaly in any longitude sector.

4. Discussion

[29] A good starting point for this discussion is the winter anomaly, as this presents problems because local observations cannot readily separate it from the annual asymmetry or anomaly. The discovery of the winter anomaly occurred with such local observations [*Berkner et al.*, 1936]. Winter values of N_mF_2 were much greater than summer ones and this was attributed to a seasonal variation of the ionosphere above the observing station. This, in turn, lead to attempts to explain the phenomenon in terms of how seasonal variations of ionospheric and thermospheric processes might give rise to this anomaly and then lead to attempts to understand composition in the thermosphere. However, the winter anomaly could also

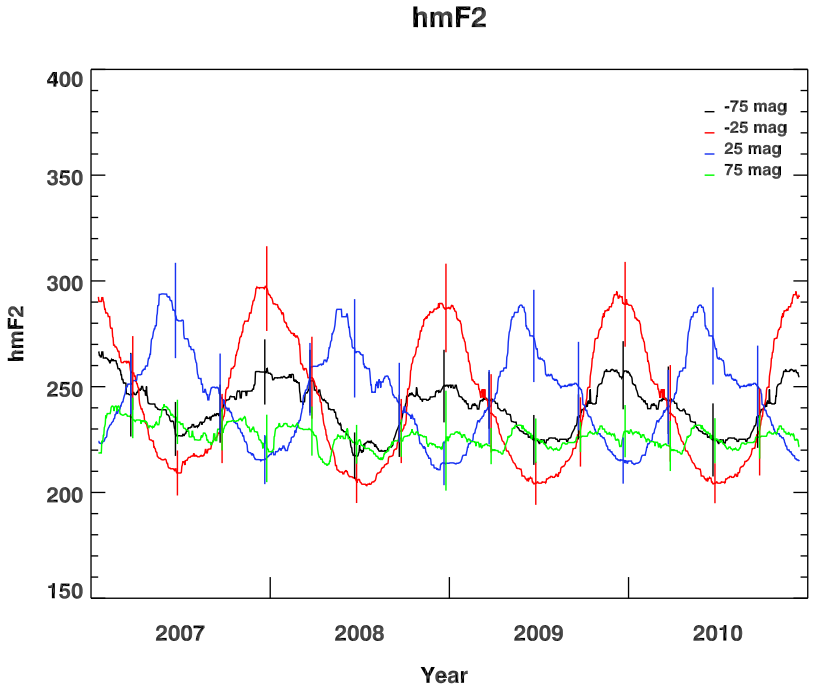

Figure 5. Line plots of h_mF_2 for four selected magnetic latitudes for the years 2007–2010. The vertical bars represent uncertainties calculated using MADs (see Section 2).

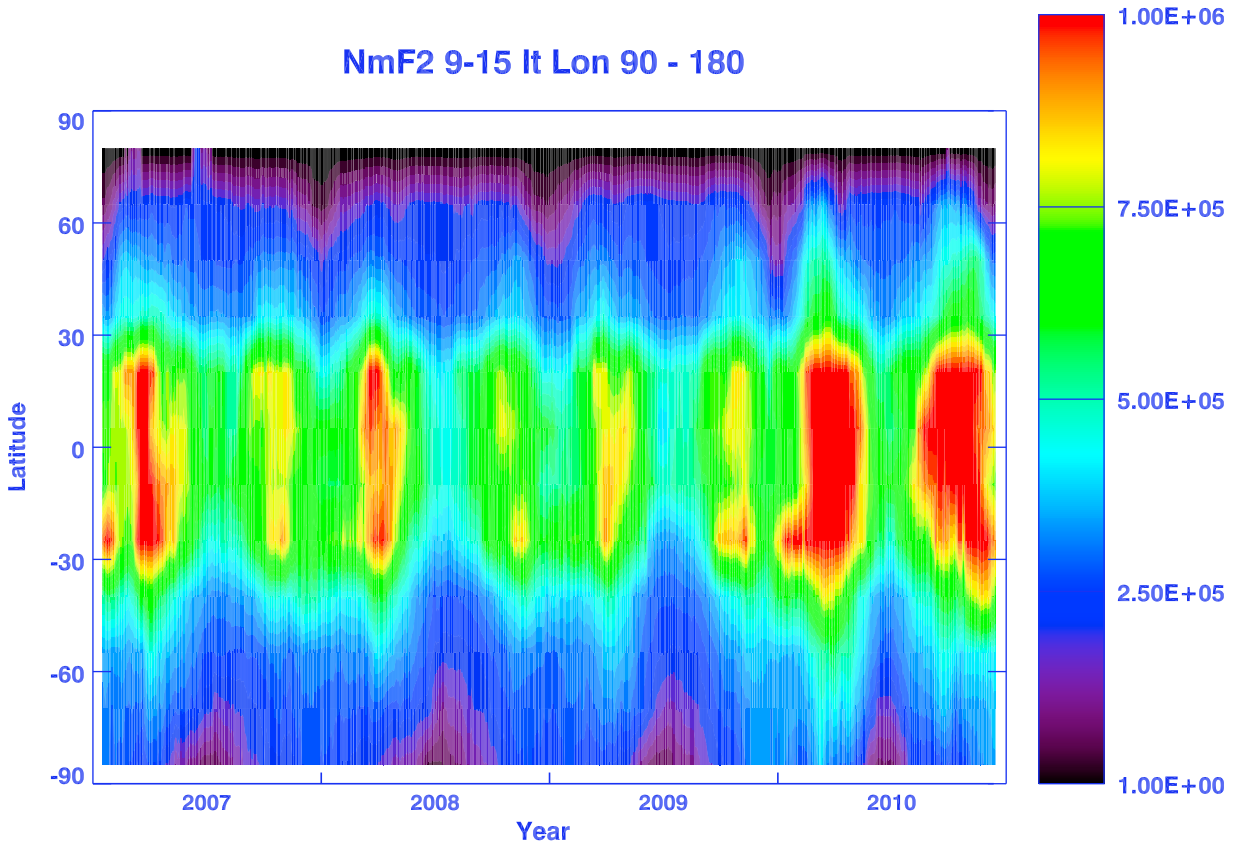

Figure 6. Thirty day medians of N_mF_2 plotted against magnetic latitude for the 90–180 longitude bin from 2007 to 2010. Unlike Figure 2 the magnetic latitude bins are 15 degrees wide.

be defined in terms of the difference in N_mF_2 at two conjugate points at the same time in the same solstice period. This definition is more applicable when composition variations are considered.

[30] Thus, there are two possible definitions of the winter anomaly: the winter to summer differences that were seen at a single northern hemisphere station [*Berkner et al.*, 1936], or the potentially composition-driven, winter-to-summer comparison that would involve simultaneously comparing conjugate points between the two hemispheres during the solstices. We prefer the latter definition, and consider that the former definition includes both the annual asymmetry (or anomaly) and the winter or seasonal anomaly added together. For the data presented here, the former definition leads to a strong "winter anomaly" in the northern hemisphere and no "winter anomaly" in the southern hemisphere.

[31] However, by our definition, there is no winter anomaly in the results presented here. In all cases N_mF_2 is greater in the summer hemisphere than in the winter hemisphere, when simultaneous measurements are made in conjugate bins. The reasons for this lack of a winter anomaly will be considered further in a later paper that will include composition measurements from GUVI.

[32] So far this discussion has concentrated on what is not there, we now consider what is there. The dominant morphological features in the COSMIC N_mF_2 data are the equatorial anomalies, the equinoctial maxima at low and middle latitudes, the annual asymmetry (or anomaly) at the same latitudes and the annual variation of N_mF_2 at high latitudes. The last phenomenon appears to be the easiest to understand as it looks like it is the result of solar zenith angle control, however no quantitative calculation of this is made here. Also, the values of h_mF_2 in the northern high latitudes do not show this simple summer to winter variation, which suggests that either the data was contaminated in this region or that this process is more complicated than we have just stated.

[33] The equatorial anomalies [e.g., *Schunk and Nagy*, 2000; *Ram et al.*, 2009, and references therein] have been the subject of numerous studies and the results presented here can add little or nothing to this accumulated knowledge other than the observations of h_mF_2 near the magnetic equator. These have a strong seasonal pattern with the maximum value of h_mF_2 always occurring on the summer side of the magnetic equator. This is consistent with the height of the F_2 peak being controlled by winds near the magnetic equator. In this scenario the winds blowing from summer to winter would raise the F_2 peak on the summer side of the magnetic equator and lower it on the winter side. Other possible causes such as the neutral temperature being greater on one side of the magnetic equator than the other can be discounted as latitudinal neutral temperature gradients in this region in the daytime are typically small. The abruptness of the transition from northern to southern summer conditions does suggest that the transition period requires further study.

[34] The equinoctial anomalies have also been intensively studied [e.g., *Rishbeth*, 1998], but the results presented here offer a new perspective on them as they present a high cadence global view of their morphology. The most unexpected results

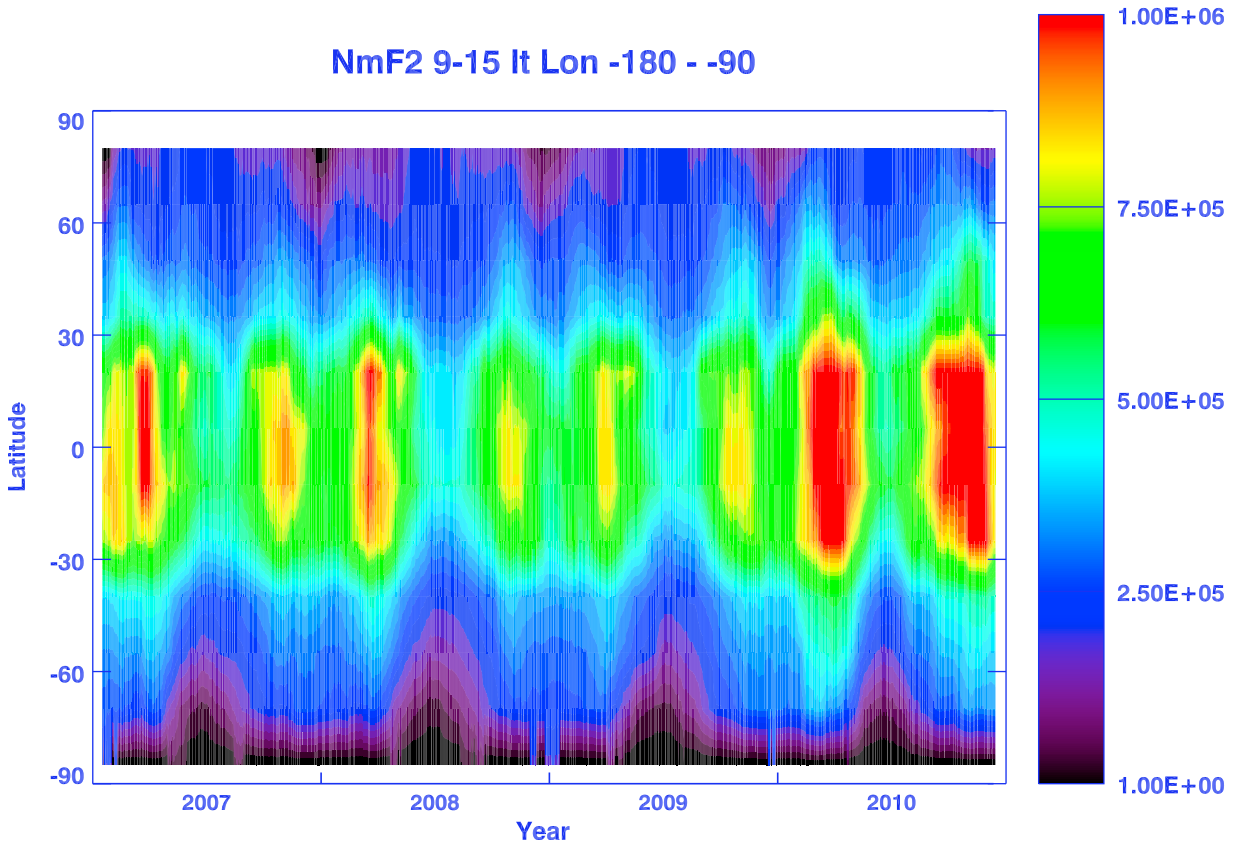

Figure 7. Thirty day medians of N_mF_2 plotted against magnetic latitude for the −180−−90 longitude bin from 2007 to 2010. Unlike Figure 2 the magnetic latitude bins are 15 degrees wide.

from this study were that their latitudinal extent varies with solar cycle, that they appeared to be centered on the magnetic equator (which would not be expected if they were high latitude phenomena), and that the second equinoctial peak appears consistently in October, rather than September. *Rishbeth* [1998], following *Ivanov-Kholodnii* [1973], listed a number of mechanisms by which they might be formed and made arguments for and against these mechanisms. It is worth considering how these new results impact these mechanisms:

[35] 1) The equinoctial maxima of neutral density.

[36] 2) The equinoctial peaks in geomagnetic activity.

[37] 3) Semi-annual oscillations in the lower or middle atmosphere.

[38] 4) The semi-annual effect in the height of h_mF_2. *Rishbeth* [1998] also listed another theory.

[39] 5) *Millward et al.* [1996] postulated an explanation depending on the location of the downwelling region where the interface between high latitude convection pattern and low latitude solar driven forcing occurs. In this explanation equinox N_mF_2 values are large because of the balance between composition changes and the solar zenith angle.

[40] *Rishbeth* [1998] also suggested an addition to 1) based on the work that *Fuller-Rowell* [1998] did on the thermospheric spoon.

[41] There are a couple of clues in the results that we have presented that influence understanding of these equinoctial peaks. First, unlike the *Becker* [1967] results, we found no semi-annual effect in h_mF_2 in the global COSMIC data set. This is not to imply that it does not exist locally, but it is unlikely that mechanism 4 has much influence on the global equinoctial peaks of N_mF_2.

[42] Second, there is no indication that the equinoctial peaks are forced directly from high latitudes. There was very little change in EUV radiation between 2007 and 2008, yet geomagnetic activity was considerably lower in the second half of 2008 as the corotating interaction region (CIR) driven storms largely disappeared in this later time period [*Burns et al.*, 2012]. More importantly, the arguments made against this mechanism by *Rishbeth* [1998] hold. Also against it is that the equinoctial peaks in geomagnetic forcing did not occur after the beginning of the downward phase of this past solar cycle [*Luan et al.*, 2009], in which our data were measured, so there is no geomagnetic forcing mechanism in this period which could produce equinoctial peaks.

[43] The current results differ from those of *Zhang et al.* [2010] insofar as there is no evidence of a semiannual variation at high geomagnetic latitudes (like Svalbard, Sondrestrom and Poker Flat) in the plots presented here. It is often difficult to compare individual stations with global data sets. In the *Zhang et al.* [2010] paper the data sets for Svalbard and Sondrestrom, which have the same geomagnetic latitude, do not have equinoctial variations in common. In Svalbard the peaks occur on about day 120 and day 225, whereas in Sondrestrom they occur on day 80 and day 250. Given that these two stations occur in the same bin in Figure 2 (which is 10 degrees of geomagnetic latitude and 360 degrees of longitude), for example, it is probable that the effects at Sondrestrom would be offset by those at Svalbard

and that a net summer maximum would appear in the COSMIC observations, as it does. This indicates that the equinoctial peaks are probably not a consistent global phenomenon at these high geomagnetic latitudes. The lack of association of equinoctial peaks with geomagnetic activity in that descending solar cycle [*Luan et al.*, 2009] also indicates that the origin of those peaks is unlikely to be due to high latitude forcing, so other aspects of *Rishbeth* [1998]'s ideas must be invoked for an explanation.

[44] Third, solar cycle variations of the latitudinal extent of the semiannual anomaly (which is also contained in a figure from *Torr and Torr* [1973] albeit in a less straightforward way) put strong constraints on possible forcing mechanisms. The absence of semiannual effects at high middle latitudes in 2007 through to the middle of 2009 indicates that a connection with high latitude forcing is unlikely, whereas the rapid expansion of the latitude range in late 2009 and 2010 suggests that the effect is very sensitive to EUV radiation, probably in association with other changes in the thermosphere and ionosphere. The timing of the second peak in October seems very important, as is its regularity. This indicates that the semiannual anomaly is not truly semiannual and also the cause is not a regular wave-like phenomenon.

[45] The annual asymmetry or anomaly vies with the equinoctial anomalies as the major source of variability in the plots. Like the equinoctial anomalies the latitudinal extent of the annual anomaly varies over the four years studied. In 2008 and 2009 it was associated more with the low-middle latitudes than with the high latitudes, which is consistent with the explanation given for it by *Zeng et al.* [2008], who indicated that the annual asymmetry is connected to the position of the geomagnetic equator relative to the geographic one. There is also evidence of the annual anomaly or asymmetry in the h_mF_2 data as the annual variations of h_mF_2 in the southern middle latitudes is much greater than that in the northern hemisphere. In other words the F_2 peak is higher in the December solstice than the June solstice at middle latitudes. This annual variation in h_mF_2 extends to higher latitudes than the annual variation of N_mF_2 appears to do.

[46] Other features are also apparent in the Figures 2 and 3. Maximum values of N_mF_2 decrease from 2007 down to a minimum in late 2008 and early 2009 and then increase greatly in 2010. This is consistent with the behavior of EUV radiation described by *Solomon et al.* [2010, 2012], but is not completely consistent with F10.7 measurements, which essentially "bottomed out" early in 2007 and did not increase until very late in 2009. A similar pattern is seen in h_mF_2 at middle latitudes. Another important feature is the symmetry of the northern and southern variations in the Figures 2 and 3. This suggests that N_mF_2 and h_mF_2 are better ordered in magnetic coordinates rather than geographic ones for the climatological data presented here.

[47] An issue with these studies is what effect the use of medians has had on our understanding of the phenomena described in this paper. The consistency of the results over time suggests that the relatively small sample size (of the order of 25 points per bin, not including the 30 day running median) does not have a major impact by introducing longitudinal biases. This also suggests that the use of medians is a robust way to approach the problem of small data samples in these COSMIC data. However, the plots do represent the base morphology of the ionosphere, rather than the variations that a station and a particular latitude and longitude might see, and thus represent the globally reproducible effects of the various phenomena rather than their local impact. We intend to push the analysis techniques further to see if we can obtain at least coarse longitudinal results from the COSMIC database to better understand the longitudinal variations of these various anomalies.

5. Conclusions

[48] COSMIC data were analyzed to obtain latitudinal medians of N_mF_2 and h_mF_2 for a set of 18 magnetic latitude bins between 0900 and 1500 local solar time. A number of phenomena were observed including:

[49] 1) There was no evidence of a winter anomaly in the data provided that it is defined as the situation where the winter values of N_mF_2 are greater than those at the conjugate latitude in the summer hemisphere. In all cases the summer values of NmF2 were greater than the winter ones at high and middle latitudes.

[50] 2) Low latitude variability is dominated by the annual anomaly or asymmetry and the equinoctial anomalies. This variability extended into the middle latitudes in 2008 and 2009 and into the high middle latitudes in 2010, indicating that these phenomena are low latitudes ones which are controlled significantly by variations in EUV radiation over the solar cycle. The annual anomaly is much stronger in the southern hemisphere than it is in the northern hemisphere.

[51] 3) The second equinoctial peak occurs in October rather than September, whereas the first one occurs in March. This argues against a semi-annual oscillation explanation for the "equinoctial" peaks in NmF2. It is clear, however, that the equinoctial peaks are not forced from the high latitudes.

[52] 4) There were no equinox peaks in geomagnetic activity during this period, so this also cannot be regarded as the cause of the equinoctial anomaly.

[53] 5) N_mF_2 an h_mF_2 vary throughout the solar minimum period in a way that suggests that EUV radiation control is continuing even as F10.7 control "bottoms out."

[54] 6) The symmetry of the effects in magnetic space suggests that the primary control of N_mF_2 and h_mF_2 is geomagnetic rather than geographic.

[55] **Acknowledgments.** We thank the COSMIC team and the COSMIC Data Analysis and Archive Center for measuring and providing access to the data used in this study. We would also like to acknowledge the support of NASA grant NNX10AQ49G from the NASA Guest Investigator Program, and NASA LWS grants NNX08AQ91G, NNX09AJ60G, and NNX10AQ59G. Additional support came from the Center for Integrated Space Weather Modeling (CISM), which is funded by the National Science Foundation's STC program under agreement ATM-0120950. NCAR is sponsored by the National Science Foundation.

[56] Robert Lysak thanks the reviewers for their assistance in evaluating this paper.

References

Appleton, E. V. (1946), Two anomalies in the ionosphere, *Nature*, *157*, 691.

Appleton, E. V., and M. A. F. Barnett (1925), Local reflection of wireless waves from the upper atmosphere, *Nature*, *115*, 333–334.

Becker, W. (1967), The temperature of the *F* region deduced from electron number density profiles, *J. Geophys. Res.*, *72*, 2001–2006.

Bellchambers, W. H., and W. R. Piggott (1958), Ionospheric measurements made at Halley Bay, *Nature*, *188*, 1596–1597.

Berkner, L. V., H. W. Wells, and S. L. Seaton (1936), Characteristics of the upper region of the ionosphere, *Terr. Magn. Atmos. Electr.*, *41*, 173–184.

Bilitza, D., and B. Reinisch (2008), International Reference Ionosphere 2007: Improvements and new parameters, *Adv. Space Res.*, *42*(4), 599–609, doi:10.1016/j.asr.2007.07.048.

Brace, L. H. (1998), Langmuir probe measurements in the ionosphere, in *Measurement Techniques in Space Plasmas: Particles*, *Geophys. Monogr. Ser.*, vol. 102, edited by F. Pfaff, E. Borovsky, and T. Young, pp. 23–35, AGU, Washington, D. C.

Burns, A. G., Z. Zeng, W. Wang, J. Lei, S. C. Solomon, A. D. Richmond, T. L. Killeen, and Y.-H. Kuo (2008), Behavior of the F_2 peak ionosphere over the South Pacific at dusk during quiet summer conditions from COSMIC data, *J. Geophys. Res.*, *113*, A12305, doi:10.1029/2008JA013308.

Burns, A. G., S. C. Solomon, W. Wang, G. Jee, C. H. Lin, C. Rocken, and Y. H. Kuo (2011), The summer evening anomaly and conjugate effects, *J. Geophys. Res.*, *116*, A01311, doi:10.1029/2010JA015648.

Burns, A. G., S. C. Solomon, L. Qian, W. Wang, B. A. Emery, M. Wiltberger, and D. R. Weimer (2012), The effects of corotating interaction region/high speed stream storms on the thermosphere and ionosphere during the last solar minimum, *J. Atmos. Sol. Terr. Phys.*, *83*, 79–87.

Chapman, J. H. (1964), Alouette topside sounder satellite—Experiment, data and results, *J. Spacecr. Rockets*, *1*(6), 684–686.

Coster, A. J., J. C. Foster, and P. J. Erickson (2003), Space weather: Monitoring the ionosphere with GPS, *GPS World*, *14*, 42–49.

Evans, J. V. (1965), Ionospheric backscatter observations at Millstone Hill, *Planet. Space Sci.*, *13*, 1031–1074.

Fuller-Rowell, T. J. (1998), The "thermospheric spoon": A mechanism for the semiannual density variation, *J. Geophys. Res.*, *103*(A3), 3951–3956.

Hajj, G. A., and L. J. Romans (1998), Ionospheric electron density profiles obtained with the Global Positioning System: Results from the GPS/MET experiment, *Radio Sci.*, *33*, 175–190.

Hoaglin, D. C., F. Mosteller, and J. W. Tukey (1983), *Understanding Robust and Exploratory Data Analysis*, Wiley, New York.

Huang, X. Q., B. W. Reinisch, D. Bilitza, and R. F. Benson (2002), New data on the topside electron density distribution, *Ann. Geophys.*, *45*, 125–130.

Ivanov-Kholodnii, G. S. (1973), Semiannual variations in aeronomy and geomagnetism, *Geomagn. Aeron., Engl. Transl.*, *13*, 823–829.

Kumar, M. (2006), New satellite constellation uses radio occultation to monitor space weather, *Space Weather*, *4*, S05003, doi:10.1029/2006SW000247.

Lei, J., et al. (2007), Comparison of COSMIC ionospheric measurements with ground based observations and model predictions: Preliminary results, *J. Geophys. Res.*, *112*, A07308, doi:10.1029/2006JA012240.

Luan, X., W. Wang, A. G. Burns, S. C. Solomon, Y. Zhang, and L. J. Paxton (2009), The peculiar declining phase of solar cycle 23: Weak semi-annual variations of hemispheric power and geomagnetic activity, *Geophys. Res. Lett.*, *36*, L22102, doi:10.1029/2009GL040825.

Millward, G. H., R. J. Moffett, S. Quegan, and T. J. Fuller-Rowell (1996), Ionospheric F-2 layer seasonal and semiannual variations, *J. Geophys. Res.*, *101*, 5149–5156.

Prölss, G. W., and U. von Zahn (1974), ESRO 4 gas analyser results: 2. Direct measurements of changes in the neutral composition during a geomagnetic storm, *J. Geophys. Res.*, *79*, 2535–2539.

Ram, S. T., S.-Y. Su, and C. H. Liu (2009), FORMOSAT-3/COSMIC observations of seasonal and longitudinal variations of equatorial ionization anomaly and its interhemispheric asymmetry during the solar minimum period, *J. Geophys. Res.*, *114*, A06311, doi:10.1029/2008JA013880.

Richmond, A. D. (1995), Ionospheric electrodynamics using magnetic apex coordinates, *J. Geomagn. Geoelectr.*, *47*, 191–212.

Rishbeth, H. (1998), How the thermospheric circulation affects the ionospheric F2-layer, *J. Atmos. Sol. Terr. Phys.*, *60*, 1385–1402.

Rishbeth, H., and C. S. G. K. Setty (1961), The F Layer at sunrise, *J. Atmos. Terr. Phys.*, *21*, 263–276.

Rocken, C., Y.-H. Kuo, W. Schreiner, D. Hunt, S. Sokolovskiy, and C. McCormick (2000), COSMIC system description, *Terr. Atmos. Oceanic Sci.*, *11*, 21–52.

Schreiner, W. S., S. V. Sokolovskiy, C. Rocken, and D. C. Hunt (1999), Analysis and validation of GPS/MET radio occultation data in the ionosphere, *Radio Sci.*, *34*(4), 949–966.

Schunk, R. W., and A. F. Nagy (2000), *Ionospheres*, Cambridge Univ. Press, New York.

Solomon, S. C., T. N. Woods, L. V. Didkovsky, J. T. Emmert, and L. Qian (2010), Anomalously low solar extreme-ultraviolet irradiance and thermospheric density during solar minimum, *Geophys. Res. Lett.*, *37*, L16103, doi:10.1029/2010GL044468.

Solomon, S. C., A. G. Burns, B. A. Emery, M. G. Mlynczak, L. Qian, W. Wang, D. R. Weimer, and M. Wiltberger (2012), Modeling studies of the impact of high-speed streams and co-rotating interaction regions on the thermosphere-ionosphere, *J. Geophys. Res.*, *117*, A00L11, doi:10.1029/2011JA017417.

Torr, M. R., and D. G. Torr (1973), The seasonal behavior of the F2-layer of the ionosphere, *J. Atmos. Terr. Phys.*, *35*, 2237–2251.

Yue, X., W. S. Schreiner, J. Lei, S. V. Sokolovsky, C. Rocken, D. C. Hunt, and Y. H. Kuo (2010), Error analysis of Abel retrieved electron density profiles from radio occultation measurements, *Ann. Geophys.*, *28*, 217–222.

Yunck, T. P., C.-H. Liu, and R. Ware (2000), A history of GPS sounding, *Terr. Atmos. Oceanic Sci.*, *11*(1), 1–20.

Zeng, Z., A. G. Burns, W. Wang, J. Lei, S. C. Solomon, S. Syndergaard, L. Qian, and Y.-H. Kuo (2008), Ionospheric annual asymmetry observed by the COSMIC radio occultation measurements and simulated by the TIEGCM, *J. Geophys. Res.*, *113*, A07305, doi:10.1029/2007JA012897.

Zhang, S.-R., J. M. Holt, A. P. Van Eyken, C. Heinselman, and M. McCready (2010), IPY observations of ionospheric yearly variations from high- to middle-latitude incoherent scatter radars, *J. Geophys. Res.*, *115*, A03303, doi:10.1029/2009JA014327.